

EROSION CHARACTERISTICS OF A MEDIUM SAND BREACHED EMBANKMENT

Zainab Mohamed Yusof*, Syura Fazreen Hamzah¹ & Shahabuddin Amerudin²

¹ Department of Hydraulics and Hydrology, Faculty of Civil Engineering, Universiti Teknologi Malaysia, 81310 UTM Johor Bahru, Malaysia

² Department of Geoinformation, Faculty of Geoinformation and Real Estate, Universiti Teknologi Malaysia, 81310 UTM Johor Bahru, Malaysia

*Corresponding Author: zainabyusof@utm.my

Abstract: Embankment breaching dam studies have been carried out since 1980s and researchers who carried out physical experiments have contributed the understanding in the breaching process. This includes lacking in data and understanding in upgrading the breach models. Therefore, this study is to analyse erosion characteristics of a medium sand of embankment breaching due to overtopping and to produce the breached outflow hydrographs for different inflow rates. Parameters such as sediment sizes, embankment slope and inflow rates were applied to examine the effects of breach parameters towards the breaching process. Experimental works on the breaching embankment were conducted to collect data needed and a dimensional analysis was proposed to get relationship of the dominant parameters that affect the failure of the embankment. The result obtained was presented in hydrographs analysis and a combination of dimensionless group of breached erosion. The finding concluded that the finer sediment produces higher peak outflow compared to a medium sediment size and controlling parameters such as particle diameter, d_{50} , velocity, u_b , and water density, ρ_w are the significant parameters that affect the process of embankment breached. It also observed that the velocity after the breaching process increases once the water flow through an embankment dam and it started to decrease after passing through the middle of embankment due to the large surface area.

Keywords: Breaching process, breach outflow hydrograph, sediment size, medium size of sediment, and breach erosion.

1.0 Introduction

Dams are massive barriers built across rivers and streams to confine and utilize the flow of water for human purposes such as irrigation and generation of hydroelectricity. This confinement of water creates lakes or reservoirs. Earthen dam are subjected to possible

failure from either overtopping or piping water, which erodes a breach through the dam. However, overtopping is very crucial for the embankment type due to the fact that the embankment dam material is eroded very quickly once the embankment is overtopped and causes a breaching by floods that exceed the capacity of the dam. Therefore, earthen dam failure has become a subject of increasing concern among dam engineers, federal, state, and local officials, and society at large.

In facts, breach simulation and prediction are always with greatest uncertainties on aspects forecasting of dam breach flooding and the uncertainty requires researchers to improve their knowledge on the dam breach. The lack of understanding of in the dam breach process is contributed by limited number of reported real dam failure events and limited number of available breach data and parameters involved. The breach parameters involved in this analysis are breach depth, breach width and breach side slope.

To overcome the issues, investigations on the breaching embankment study have been carried out since 1980s and researchers who carried out physical experiments have contributed in understanding the breach process. However, there are still lacking in data and understanding in upgrading the breach models. The objectives of this study are to determine the erosion characteristics of medium sand and to produce a breached hydrographs. Experimental investigation on dam breaching study was conducted using a physical straight channel in Hydraulics and Hydrology Laboratory at Universiti Teknologi Malaysia, UTM Johor Bahru.

2.0 Embankment Breaching

The predominant mechanism of breaching for earth-filled embankment is by erosion of the embankment material due to flow of water either over or through the dam. In this study, an overtopping of the embankment is one of the causes that can initiate erosion type breaches. The breaching characteristics needed as input are the size of embankment, shape of the dam breach, the time that is required for the breaching to develop and the reservoir water surface elevation at which breaching begins. These characteristics are dependent, to a large extent, on the breach forming that was classified into two general categories: (1) Breaches formed by the sudden removal of a portion or all of the embankment structure as a result of overstressing forces on the structure and (2) breaches formed by erosion of the embankment material.

In addition, experimental works are required so that the results from the numerical modeling can be verified. These works have been carried out since the end of 1980's (Zhu *et. al*, 2006). These experimental works including large scale tests and small scale tests conducted either in laboratory or field site. Small scale models are useful in the contribution to understand the process of breach, as well as the geometry of final breach

(Franca *et. al*, 2000). Indeed, laboratory works have been done to help engineers and researchers in establishing the knowledge on the embankment dam breach process. Laboratory works may involve various parameters such as sediment size, compaction effort, size of embankment, embankment height, and inflow rate. Most of the study varied the parameters in order to study their effects on the breach process, as well as to understand the breach progress in details.

In an embankment breaching study, there are two main primary tasks involved, which are 1) prediction of the outlet hydrograph, and 2) routing of the hydrograph through the downstream valley (Wahl, 1998). Ralston (1987) has discussed the mechanics of embankment erosion from overtopping. For non-cohesive embankments, materials are removed from the embankment in layers by tractive stresses. The erosion process from overtopping begins at a point where the tractive shear stress exceeds a critical resistance that keeps the material in place. For cohesive embankments, breaching takes place by head cutting. Usually, a headcut initiates near the downstream toe of the dam, and then advances upstream until the crest of the dam is breached. Figure 1 shows the erosion embankment materials due to overtopping (Chen, 2015).

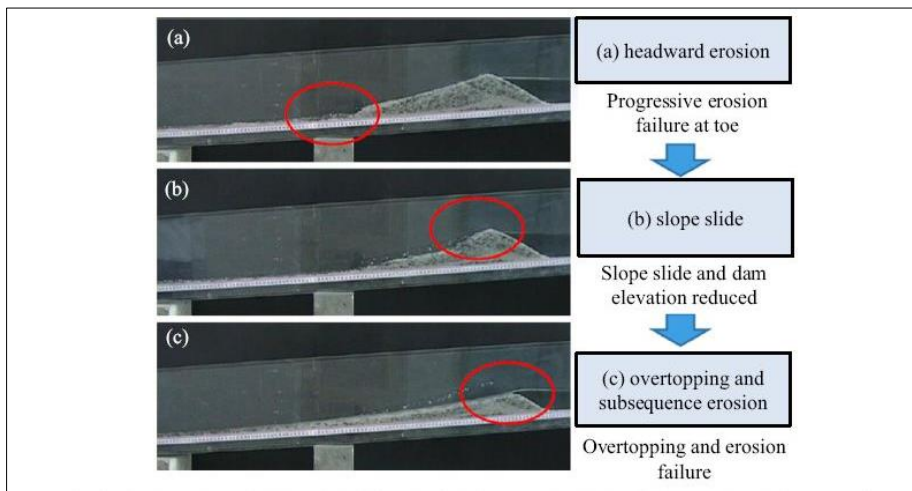


Figure 1: Embankment breaching process in a complex of failure mode in the flume test (Chen, 2015)

In Figure 2 shows the breach erosion process during failure due to overtopping (Johnson *et. al*, 1976). If the foundation is reached the breach is V-shaped and approximately three to four times as wide as deep. While the foundation is often a non-erodible zone, the erosion proceeds in lateral direction. This process continues until the reservoir is empty or the velocity of the outflowing water is too low to erode the embankment any further.

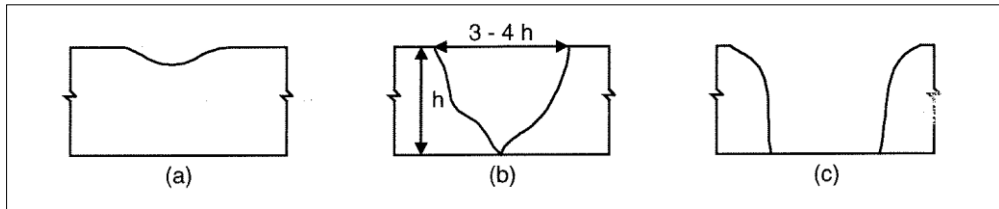


Figure 2: Breach erosion process during failure due to overtopping (Johnson *et al.*, 1976)

The flow regimes and erosion zones of overtopped embankments was studied by (Powledge *et al.*, 1989) They found three zones of embankment erosion due to overtopped flow, as illustrated in Figure 3. Zone 1 was region where less erosion might happen due to subcritical flow approaching the embankment, and the flow velocities and shear stresses above the crest are relatively low. Further along the crest, a so-called transition zone from subcritical to critical flow observed (Zone 2). This zone exhibited high stresses due to the changes of energy slope. Zone 3 was an area with high potential of erosion. The flow started to accelerate rapidly along the downstream slope, resulting in increased shear stresses at the downstream corner of the crest.

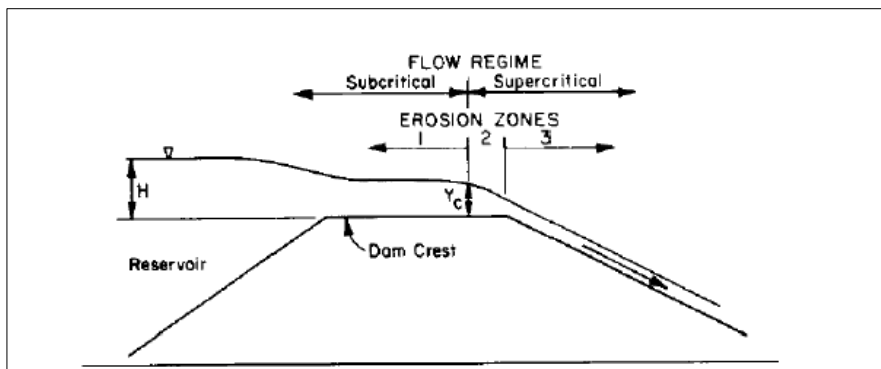


Figure 3: Flow regimes of overtopped (Powledge *et al.*, 1989)

3.0 Experimental Setup

This study was carried out based on experimental work in the laboratory to collect the data needed and used to analyze the flow and get the erosion characteristics due to dam breaching and produce outflow hydrograph. The process can be explained from the flow chart shown in Figure 4. Various parameters such as sediment sizes, embankment slope and inflow rates were used to study the effects breach parameters towards its process.

A sieve analysis was conducted to get the medium grain size which was in the range of 0.25 mm to 0.5 mm. The medium grain size was used as the embankment dam materials. The experimental was tested for two different inflow rates through the V-notch, which are $Q_1 = 0.8 \times 10^{-3} \text{ m}^3/\text{s}$ and $Q_2 = 1.2 \times 10^{-3} \text{ m}^3/\text{s}$ and the discharged value was calibrated by using a miniature and electromagnetic flow meter (EFM) as depicted in Figure 5 and Figure 6. A physical model was setup in the laboratory as shown in Figure 7 and Figure 8 shows the schematic diagram of the experimental setup used.

The test was carried out in a flume of 11 m long, 0.6 m deep and 0.61 m wide. The wall of the flume is installed transparent at one side for observation and recording work during the tests. Figure 9 shows the embankment setup when the compaction work has completed. At the center on embankment crest, a notch was produced which is marked as a circled. It functioned as a weak point of the embankment dam. The notch size was 1.7 cm height and 6.5 cm width. The details study of the experiment as follows,

1. Medium grain size in range 0.25mm to 0.5mm of an embankment dam with medium sand and slope of 1V:2H.
2. The top part of the embankment dam as in Figure 10 was coloured by green to differentiate the soil that will be transported during the failure and to measure the distance of deposition due to breaching event for the coloured sand.
3. Two different inflow rates were applied, which were $Q_1 = 0.8 \times 10^{-3} \text{ m}^3/\text{s}$ and $Q_2 = 1.2 \times 10^{-3} \text{ m}^3/\text{s}$.

The flume was kept horizontally throughout the experiment. Railing was installed on both side of the channel. At the end of the flume outlet, a V-notch was installed to measure the outflow discharge after the breach process. The whole breaching process for the whole test was recorded using video recorders.

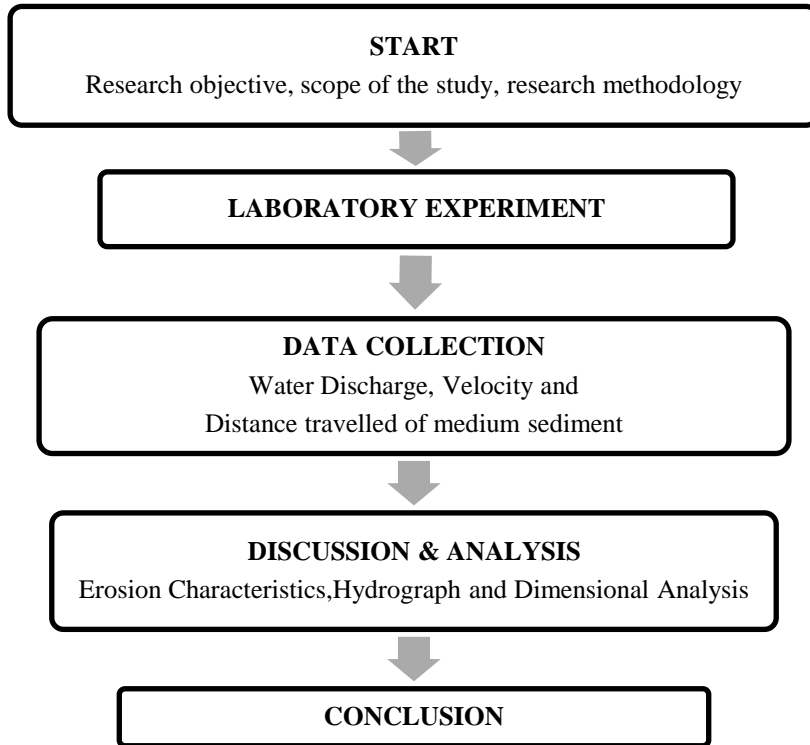


Figure 4: A flow chart of the experimental setup.



Figure 5: Flow measurement (a) a V-notch at the outlet, and (b) a point gauge to record water levels.



Figure 6: Flow calibration; (a) a miniature velocity, and (b) an Electromagnetic Flow Meter (EFM).



Figure 7: An embankment setup in the channel.

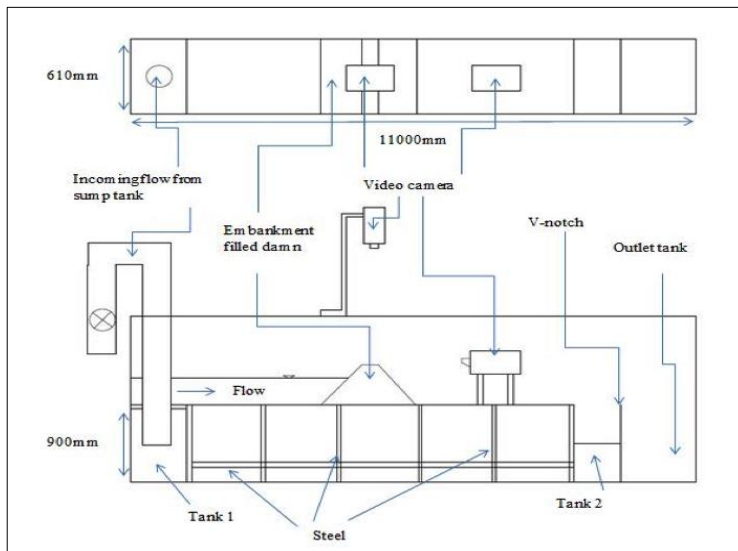


Figure 8 : Schematic layout of the flume (in mm); Top: Plan view and Bottom: Side view.



Figure 9: A notch; acting as a weak point of the embankment dam, is located at the middle of the embankment filled.

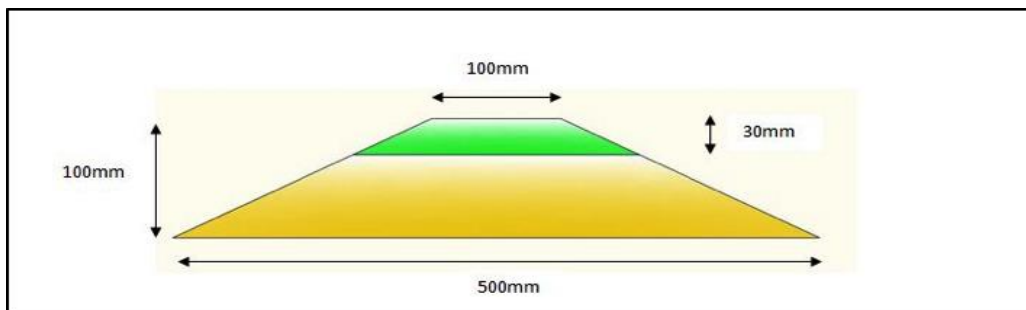


Figure 10: A schematic diagram of an embankment dam size. A medium grain size was used (0.25 mm – 0.5mm). A green thin layer of 30 mm was compacted onto the top of embankment so that the sediment movement could be seen clearly in the water.

3.1 Experimental Procedures

As mentioned, the experimental study includes hydraulics and geotechnical aspects, especially the properties of the soil material. In the present study, the inflow rates were given as $Q_1 = 0.8 \times 10^{-3} \text{ m}^3/\text{s}$ and $Q_2 = 1.2 \times 10^{-3} \text{ m}^3/\text{s}$ respectively. The video cameras were used to record the temporal deposition of the crest (colored) of embankment due to an embankment erosion process.

During the reservoir filling process, water was pumping into the flume from the sump tank. The sump tank pumps the water based on the valve opening, which has been tested

and calibrated. Water will be kept constant until it reaches the notch level at the embankment crest. Once the water level reached the notch, then the stopwatch is starting to record the breaching time. The progression of the breaching and deposition will be recorded. Results of plan view and downstream view were used for further analysis to calculate the erosion rate due to dam breaching. The test was repeated three times for each inflow rates for comparison results.

4.0 Results and Discussion

4.1 Failure Modes and Breached Hydrographs

The comparison for experimental test result with two different inflow rates and sediment sizes were used in the analysis. Figure 11 shows the result of breach hydrographs by using two different inflow rates. The graph clearly showed that Q_2 produced the highest peak outflow which was $5.36 \times 10^{-3} \text{ m}^3/\text{s}$ compared to Q_1 , which is $4.35 \times 10^{-3} \text{ m}^3/\text{s}$. The time required for Q_2 to produce peak outflow was at $t = 80 \text{ s}$ which was only took around 10 s to trigger the peak time. Meanwhile Q_1 took around 80 s later than the peak time for Q_2 which was at $t = 170 \text{ s}$. It shows that, the larger inflow rates produce the shorter peak time; give the large impact on the embankment where the embankment dam is easily eroded due to higher flow velocity at the notch. As the larger inflow for Q_2 , it took shorter time to reach the steady state of flow compared to Q_1 . Figure 12 indicated breach hydrographs from the previous research by (Mat Lazin, 2013) with used similar inflow rate and sediment size which in range 0.2 mm to 0.6 mm. It can be concluded that the peak time and peak outflow for the medium sand was validated with the previous results where the bigger inflow rate will produce the shorter peak time and also took shorter time to reach the steady state of flow compared to others.

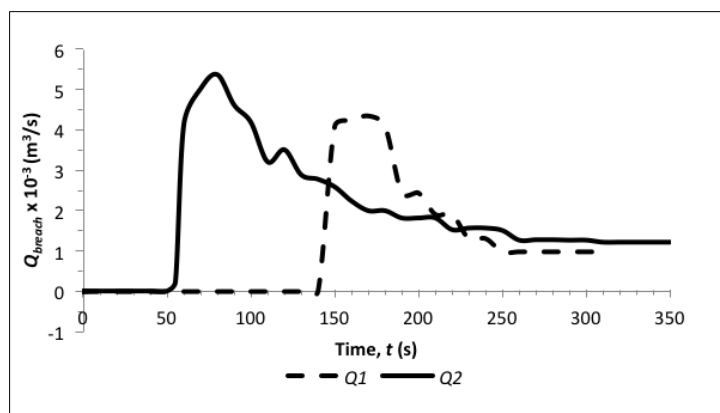


Figure 11: Breach hydrographs for different inflow rates.

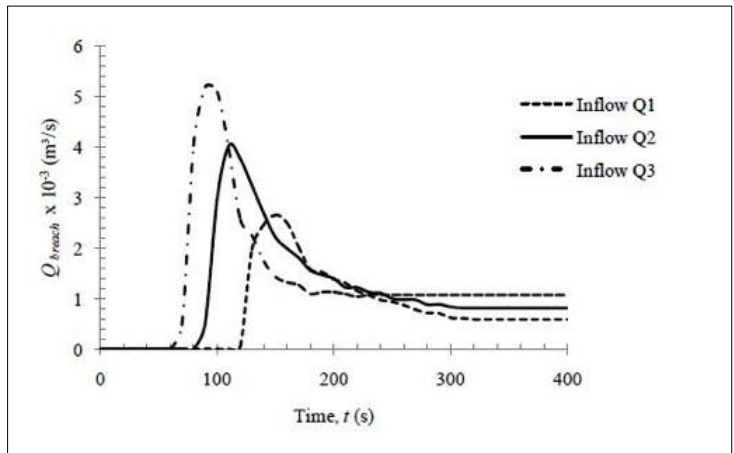


Figure 12: A comparison of Breach hydrographs (Mat Lazin, 2013). Inflow rate used for comparison was $Q_3=1.2 \times 10^{-3} \text{ m}^3/\text{s}$, which is similar with the current study.

A similar trend of hydrograph has showed in Figure 13. The result of breach hydrographs was compared with the same inflow rate, which is $Q_2 = 1.2 \times 10^{-3} \text{ m}^3/\text{s}$ but using different sizes of sediment. From the graph, it showed that for the medium sediment to reach the peak outflow, it requires 60 s faster than the finer sediment. This is due to sediment size and effect the erosion on the sediment as stated in Bhattarai *et al.*, (2014) when $t = 80 \text{ s}$, the medium sediment has reached the peak outflow while for the finer sediment which was at $t = 140 \text{ s}$. However, medium sediment produced the lowest peak outflow which was $5.36 \times 10^{-3} \text{ m}^3/\text{s}$ compared with finer sediment, $8.0 \times 10^{-3} \text{ m}^3/\text{s}$. The finer sediment seemed to be more resistive to the erosion once embankment has overtopped due to sediment size and slow saturation rate. The suction pressure acts more in finer sediment and took the longer time to develop the breach and finally collapse.

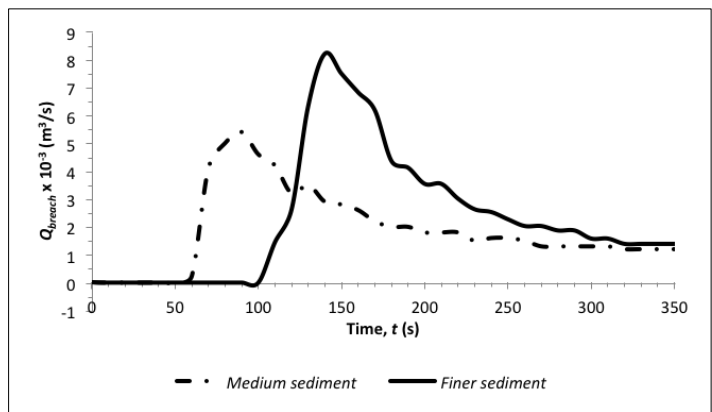


Figure 13: Breach hydrograph of different sediment sizes.

From Figure 14, it was clearly described the breach progression for $Q_2 = 1.2 \times 10^{-3} \text{ m}^3/\text{s}$ and the embankment material used was medium sand, in range 0.25 mm to 0.5 mm. The breach process was initiated when water eroded the notch area at the middle of the embankment dam. The water entered and eroded the embankment material starting from the notch area from (a) to (d) and Figure 14(e) shows how the embankment material was eroded vertically until about 90 s. Lateral erosion took place after a few seconds and started to widen the breach laterally until to the final stage of breach indicating no lateral breaching.

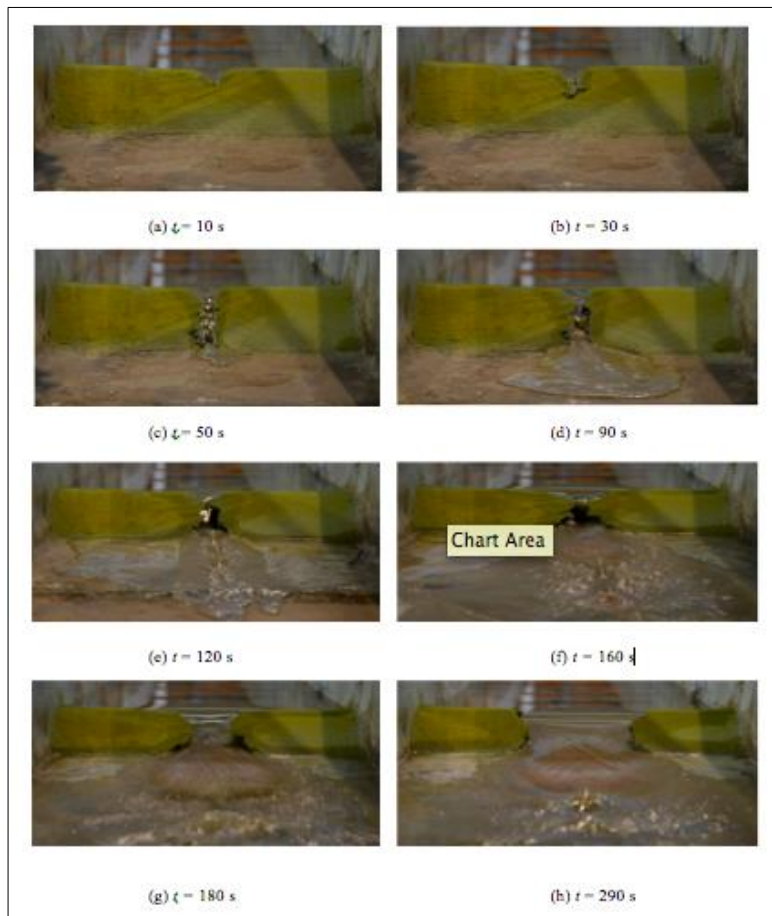


Figure 14: Temporal progression of lateral breaching for Q_2 ; (a) $t = 10 \text{ s}$, (b) $t = 30 \text{ s}$, (c) $t = 60 \text{ s}$, (d) $t = 90 \text{ s}$, (e) $t = 120 \text{ s}$, (f) $t = 160 \text{ s}$, (g) $t = 180 \text{ s}$ and (h) $t = 210 \text{ s}$.

4.2 Velocity after the Embankment Breached

Figure 15 shows the 4 points location where the velocities data were taken after the breaching process, using the Electromagnetic Flow Meter (EMF) for $Q_2 = 1.2 \times 10^{-3} \text{ m}^3/\text{s}$. There are 4 locations were chosen and the distances for each point from the middle of embankment were also recorded. The results showed that the highest velocity was located at V_3 , which is $V_3 = 0.34 \text{ m/s}$, where it was in the middle of embankment. V_1 have the lowest velocity compared to the others. The velocity is not directly proportional to the surface area of embankment after breaching; it was proven by the data collection of velocity at V_3 , which the area at V_3 is smaller than the others point. Figure 16 shows the pattern of velocity towards the distance. The velocity after the breaching process increases once the water flow through embankment dam and starts to decrease after passing through the middle of embankment due to the large surface area. It can be concluded that the higher rate of erosion for the present embankment material was occurred approximately at the point of V_3 where the larger velocity took placed.

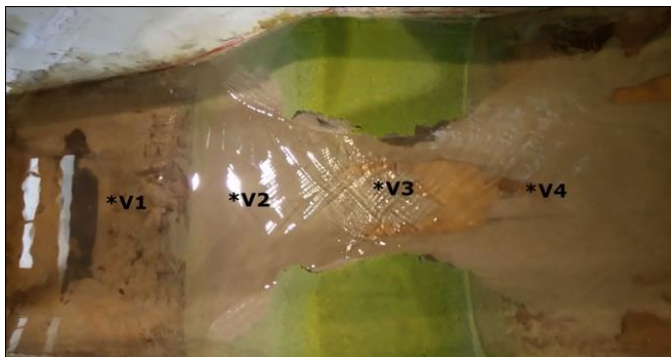


Figure 15: Locations of the velocity measurement after the embankment failed.

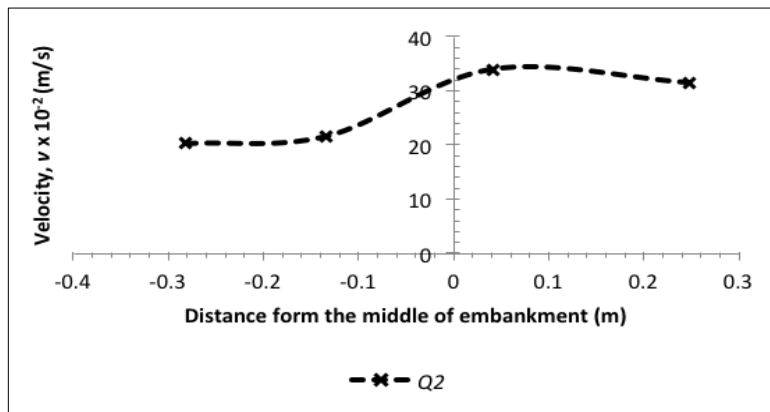


Figure 16: Flow velocities after embankment failed, for inflow rate, $Q_2 = 1.2 \times 10^{-3} \text{ m}^3/\text{s}$.

4.3 Effect of Inflow Rates and Velocity

Figure 17 shows the velocity of sediment travelled based on a different inflow rates applied to the embankment. With the large inflow, the embankment eroded faster, which then transported the soil to downstream area. The distance travelled of sediment depends on the velocity of the water flow, the large inflow rate produced high velocity and sediment travelled becomes longer. From the graph, it showed that the sediment distance travelled for Q_2 was longer than Q_1 which 3.79 m far from the embankment dam due to the velocity with a large inflow rate. The highest velocity for Q_2 was $v = 68.91 \times 10^{-3}$ m/s while Q_1 , $v = 23.4 \times 10^{-3}$ m/s. The distance sediment transported for Q_1 was 0.28 m shorter than Q_2 with the percentage difference velocity about 66%.

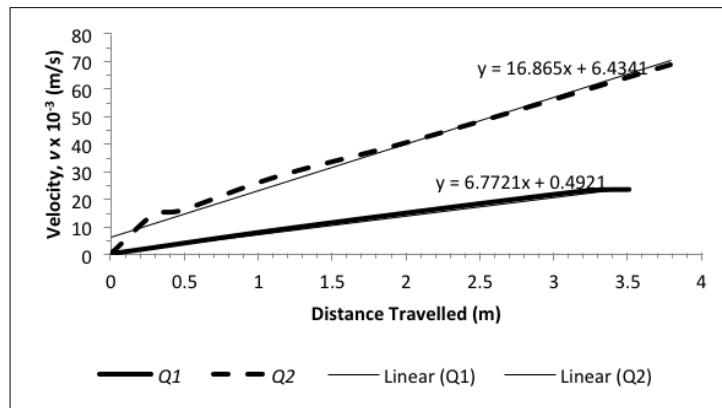


Figure 17: Velocity of sediment travelled with difference inflow rates.

A similar pattern of graph velocity against sediment travelled was observed for different grain sizes of sediment transport, as shown in Figure 18. The results indicated that the distance travelled increase with increases of velocity. However, from the comparison of difference sediment sizes it showed that even the same inflow rates applied to embankment it will produce difference velocity. This is due to the factors of volume of sediment transported, suspended load and bed load. The velocity decreases with decreasing in sediment size as showed in the graph where the finer sediment have the lowest velocity which $v = 28.4 \times 10^{-3}$ m/s compared to medium sediment, $v = 68.91 \times 10^{-3}$ m/s. Finer sediment being transported was have the shortest distance compared to medium sediment due to the velocity for each sediment where the distance travelled for finer sediment is 2.84 m far from the embankment while for medium sediment is 3.79 m.

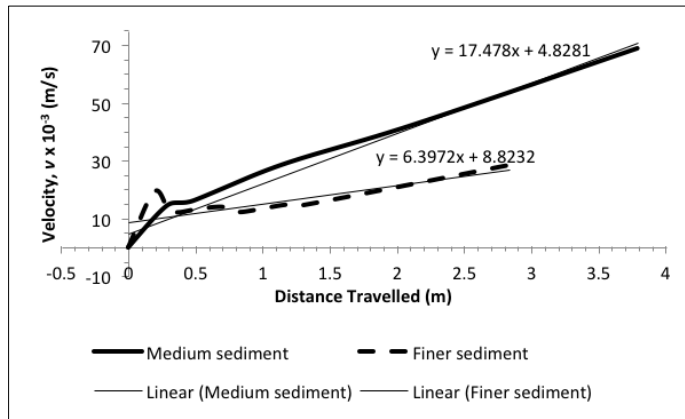


Figure 18: Velocity of sediment eroded with difference sizes.

Figure 19 was clearly indicates that Q_2 was produced the higher velocity compared to Q_1 . The time required for Q_2 to reach a maximum velocity, $v = 68.9 \times 10^{-3}$ m/s which was used for sediment transported at $t = 55$ s and it is the longer period compared to Q_1 . The velocity increases when the inflow rates increase. Thus, the erosion rate for embankment materials becomes high due to increasing of the velocity. However, Q_1 have the lowest erosion rate compared to Q_2 because the higher velocity for Q_1 , where $v = 43.4 \times 10^{-3}$ m/s and it was slightly lower than Q_2 .

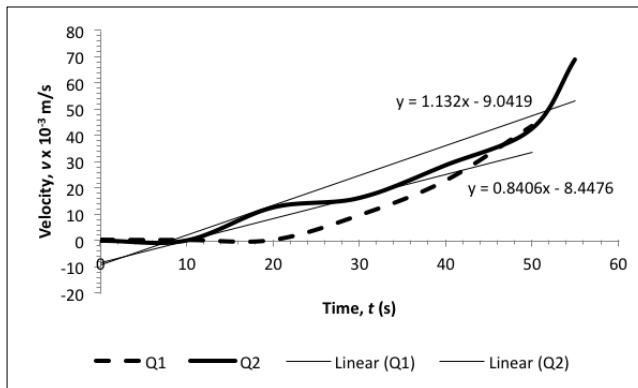


Figure 19: Erosion rate of sediment embankment with different inflow rates.

4.4 Proposed Dimensional Analysis

Dimensional analysis was used to simplifying a physical problem by appealing to dimensional homogeneity to reduce the number of relevant variables. The Buckingham

Theorem was used to analyse and determine the dimensionless group of variables for the data collections. From the experiment that was conducted, the dimensional analysis explained for each variable which related to derive a physical relationship in process of embankment dam breaching. The dimensions used in the breaching process is summarised in Table 1.

There are 10 π groups which are contributed to embankment dam breached and it can be categorised as follows,

- 1) Bank geometry
- 2) Hydraulic
- 3) Soil capacity (resistance to erosion)
- 4) Grain resistance
- 5) Others

Table 1: Dimensions for breaching process.

Variable	Unit	Dimensional
Channel slope, S_0	-	-
Channel width, B	m	L
Water depth, D	m	L
Embankment height, h_b	m	L
Embankment erosion rate, ξ	m/s	LT^{-1}
Velocity, u_b	m/s	LT^{-1}
Boundary shear stress, τ_o	N/ms^2	$ML^{-1}T^{-2}$
Critical shear stress, τ_c	N/ms^2	$ML^{-1}T^{-2}$
Particle diameter, d_{50}	m	L
Fall velocity, ω	m/s	LT^{-1}
Shear velocity, U_*	m/s	LT^{-1}
Gravity acceleration, g	m/s^2	LT^{-2}
Water density, ρ_w	kg/m^3	ML^{-3}
Embankment particle density, ρ_s	kg/m^3	ML^{-3}
Total variable, n = 13		Total dimensional, m = 3

Experimental data are very useful in presenting the mechanism with regards to erosion of dam breached and it also serve basic fundamental in developing future predictions by means of simulations in any modeling. From the data that have been collected, a physical relationship can be derived by choosing variable such as velocity, u_b , mean particle diameter, d_{50} , and water density, ρ_w as repeating variables. It is reasonable to choose these variables to be repeated because they can be directly measured in situ or through laboratory experiments or calculated leaving others as independent variables.

For π_1 :

$$\pi_1 = d_{50}^a u_b^b \rho_w^c \xi^1 \tag{1}$$

$$M^0 T^0 L^0 = [L]^a [LT^{-1}]^b [ML^{-3}]^c [LT^{-1}]^1 \tag{2}$$

$$\begin{aligned} \pi_1 &= \xi \cdot u_b^{-1} \\ &= \xi / u_b \end{aligned}$$

Groups of independent variables are as follow:

$$\Phi = \left[\frac{\xi}{u_b}, \frac{B}{d_{50}}, \frac{D}{d_{50}}, \frac{h_b}{d_{50}}, \frac{\tau_0}{\rho_w u_b^2}, \frac{\tau_c}{\rho_w u_b^2}, \frac{\omega}{u_b}, \frac{U_*}{u_b}, \frac{g}{u_b}, \frac{\rho_s}{\rho_w} \right] \tag{3}$$

$$\frac{\xi}{u_b} = f \left(\frac{B}{d_{50}}, \frac{D}{d_{50}}, \frac{h_b}{d_{50}}, \frac{\tau_0}{\rho_w u_b^2}, \frac{\tau_c}{\rho_w u_b^2}, \frac{\omega}{u_b}, \frac{U_*}{u_b}, \frac{g}{u_b}, \frac{\rho_s}{\rho_w}, S_0 \right) \tag{4}$$

The parameters provided in (4) is a functional relationship in terms of dimensionless embankment erosion rate using Buckingham Pi theorem. However the dimensionless critical shear stress $\tau_c / (\rho_w u_b^2)$ is written in terms of the critical Froude number, Fr_c at which embankment erosion is initiated. Therefore, the final results of dimensional analysis can be simplified as to:

$$\frac{\xi}{u_b} = f \left(\frac{B}{d_{50}}, \frac{D}{d_{50}}, \frac{h_b}{d_{50}}, \frac{\tau_0}{\rho_w u_b^2}, Fr_c, \frac{\omega}{u_b}, \frac{U_*}{u_b}, \frac{g}{u_b}, \frac{\rho_s}{\rho_w}, S_0 \right) \tag{5}$$

Based on the established functional relationship with regards to the embankment erosion, the dimensionless parameters were calculated into their dimensionless group following the four (4) categories as mentioned before. Table 2 shows the dimensionless group controlling parameters in embankment erosion due to breaching based on their parameter class. The importance of these parameters and their functions describing the rate of embankment erosion rationalizes the use of these parameters in the development of the new equation.

Table 2: Controlling parameters in a proposed embankment erosion

No.	Parameter Class	Dimensionless Group
1.	Hydraulic (flow resistance)	$\frac{\tau_0}{\rho_w u_b^2}, \frac{\tau_c}{\rho_s u_b^2}, \frac{\omega}{u_b}, \frac{U_*}{u_b}, \frac{g}{u_b}$
2.	Resistance capacity of soil	$\frac{\rho_s}{\rho_w}$
3.	Embankment geometry	S_0
4.	Grain resistance	$\frac{B}{d_{50}}, \frac{D}{d_{50}}, \frac{h_b}{d_{50}}$

5.0 Conclusions

This study focuses on the most common mechanism of dam failure, which is overtopping. This study aims to understand the erosion characteristics of medium sand and breached outflow hydrograph due to overtopping embankment failure. Experimental works were carried out to achieve the objectives of the study. Factors such as inflow rates and grain sediment sizes of sediment were varied and tested. The conclusion that can be drawn from the present study can be classified into the following sections:

5.1 Breached Hydrographs

Breach hydrograph consists of two main parameters in the embankment breach studies, which are peak outflow and peak time. The breach hydrograph has been carried out and the conclusions are the higher inflow rate, given the significant impact to the peak outflow and also time peak. The time required for dam to fail for bigger inflow rate was shorter than smaller inflow rate and produce the higher peak outflow. In the other hand, the finer sediment produce higher peak outflow compared to medium sediment. However, the peak time for finer sediment to arrive peak time was longer than the medium sediment.

5.2 Velocities at the Breached Area

The velocity at the breached area has been recorder after the embankment was completely eroded. It showed that the breaching process increases once the water flow through an embankment dam and it started to decrease after passing through the middle of embankment due to the large surface area.

5.3 Dimensional Analysis

From dimensional analysis it can be concluded that the most controlling parameters such as particle diameter, d_{50} , velocity, u_b , and water density, ρ_w are the significant parameters affect the process of the proposed embankment breaching.

6.0 Acknowledgements

The authors would like to thank and acknowledge the Universiti Teknologi Malaysia (UTM) and Ministry of Higher Education of Malaysia for their financial supports on the University Research Grant, Vot Number Q.J130000.2522.09H07.

References

- Franca, M.J., and Almeida, A.B. (2000). Experimental Tests on Rockfill Dam Breaching Process. *International Symposium on Hydraulic and Hydrological Aspects of Reliability and Safety of Hydraulic Structures*. May. St.Petersburg.
- Johnson, F. A and Illes, P. (1976). A classification of dam failures. *Water Power Dam Constr* 28, 43-45.
- Pawan Kumar Bhattarai, Hajime Nakagawa, Kenji Kawaike, Hao Zhang. (2014). *Experimental Study on Effect of Sediment Size on River Dyke Breach Characteristics Due to Overtopping*. Japan: Kyoto University.
- Powledge, G. R., Ralston, D. C., Miller, P., Chen, Y. H., Clopper, P. E. and Temple, D.M. (1989). *J. Hydr. Eng.*, vol. 115(8),. *Mechanics of Overflow Erosion on Embankments II: Hydraulic and Design Considerations*, 1056-1075.
- Ralston, D. C. (1987). Mechanics of embankment erosion during overflow hydraulic engineering. *Proceedings of the 1987 ASCE National Conference on Hydraulic Engineering(Williamsburg, Virginia)*, 733-738.
- Su-Chin-Chen; Tsung-Wen Lin; Chien-Yuan Chen. (2015). *Modeling of natural dam failure modes and downstream riverbed morphological changes with different dam materials in flume test*, 188(2015)148-158.
- Wahl, T.L. (1998). *Prediction of Embankment Dam Breach Parameters: A Literature Review and Needs Assessment*. Bureau of Reclamation, U.S. Dept. Of the Interior, Denver.
- Zhu, Y.H, Visser. P.J., and Vrijling, J.K. (2006). Laboratory Observations of Embankment Breaching. *The 7th International Conference on Hydrosience and Engineering*. September 10-13,2006. Philadelphia USA : Drexel University.